MiR-122-5p inhibits the epithelial mesenchymal transition of liver cancer cells by inducing hiPSCs to differentiate into hepatocyte-like cells

Qianzhe Xing,[1,2#] Yanjie Xu,[1,2,#] Ying Luo,[3] Chenglong Li,[3] Peng Wang,[3] Bin Kang,[1,2] Chengjun Lu[1,2]

[1]Department of Hepatobiliary Surgery;
[2]Tianjin Institute of Hepatobiliary Disease;
[3]Tianjin Key Laboratory of Artificial Cell, Tianjin Institute of Hepatobiliary Disease, Artificial Cell Engineering Technology Research Center of Public Health Ministry, Third Central Hospital of Tianjin, China

[#]*These authors contributed equally to this work.*

ABSTRACT

Epithelial-mesenchymal transition (EMT) is closely linked to liver cancer prognosis, invasiveness, and aggressiveness. One promising treatment for liver cancer is cell therapy, where stem cells are stimulated to develop into functional liver cells. This study aimed to investigate the effect of miR-122-5p on the differentiation of human induced pluripotent stem cells (hiPSCs) into hepatocyte-like cells and its impact on the EMT process in liver cancer cells. MiR-122-5p was overexpressed or silenced in hiPSCs to analyze the expression of liver-specific markers, including AFP, ALB and ASGPR, to confirm hepatocyte-like differentiation. A co-culture system with HepG2 liver cancer cells was also used to evaluate the effect of miR-122-5p-overexpressing hiPSCs or miR-122-5p-silencing hiPSCs on the expression of EMT markers. Results revealed that overexpression of miR-122-5p in hiPSCs induced hepatocyte-like characteristics, as evidenced by increased levels of AFP, ALB, and ASGPR. However, knockdown of miR-122-5p had the opposite effect. In the co-culture system, hiPSCs overexpressing miR-122-5p inhibited the EMT process of HepG2 cells, resulting in increased levels of mesenchymal markers and decreased levels of epithelial markers. Taken together, miR-122-5p promotes the differentiation of hiPSCs into hepatocyte-like cells and inhibits EMT process of liver cancer cells. Targeting miR-122-5p may be a novel approach to prevent liver cancer progression through cell therapy.

Key words: liver cancer; induced pluripotent stem cells; epithelial-mesenchymal transition; miRNA.

Correspondence: Chengjun Lu, MM. Department of Hepatobiliary Surgery, Third Central Hospital of Tianjin, 83 Jintang Road, Hedong District, Tianjin, China. E-mail: 15522242638@163.com

Contributions: QX, YX, CLu, study design, experiments performing; YL, CLi, data collection; PW, BK, data analysis; QX, YX, CLu, original manuscript drafting. All authors read and approved the final manuscript.

Conflicts of interest: the authors declare that they have no conflicts of interest to report regarding the present study.

Ethics approval: not applicable.

Data availability statement: the datasets used and/or analyzed during the present study are available from the corresponding author upon reasonable request.

Funding: this study was supported by the Tianjin Health Bureau Funded Project (No. 2013KR01).

Introduction

Among the top five most hazardous types of cancer globally, liver cancer is one of the most prevalent and the only type with an incidence that continues to rise annually. The incidence of liver cancer in China accounts for half of the global burden.[1] The early symptoms of liver cancer are often subtle and most liver cancer patients are diagnosed at an advanced stage, which significantly worsens their prognosis and quality of life.[2] Therefore, identifying effective therapeutic targets and strategies is crucial for liver cancer patients. An important process in tumor metastasis has been termed epithelial-mesenchymal transition (EMT), which is defined by structural changes in epithelial cells, including the loss of polarization and specialized intercellular contacts, as well as the acquisition of mesenchymal-like cell morphology and functional properties. This procedure enhances the ability of cancer cells to proliferate, migrate, and invade.[3] Given the pivotal role of EMT in the progression and metastasis of liver cancer,[4] targeting EMT inhibition in cancer cells has emerged as a major research focus.

Liver transplantation is a significant therapeutic option for liver cancer, but it is associated with a higher mortality. Hepatocellular transplantation (HCTx) is a promising alternative therapy, but the common problems faced by HCTx are the lack of available hepatocytes and the limited regenerative ability of transplanted cells.[5] Over the past few years, stem cells have attracted more interest in possible therapeutic options for liver cancer due to their high proliferative ability, low immunogenicity, and potential for multidirectional differentiation.[6] Among them, human induced pluripotent stem cells (hiPSCs) derived from fibroblasts have the ability to infinitely expand and specialize into any type of cell, and can avoid the scientific and ethical issues associated with embryonic stem cells. This is expected to address the problem of increased mortality caused by liver transplantation and make cell therapy possible.[7,8] Our preliminary research has demonstrated that serum from patients undergoing liver resection promotes the differentiation of hiPSCs into hepatocyte-like cells.[9] Furthermore, Yuan *et al.*[10] have shown that transplantation of hepatocyte-like cells derived from iPSCs improves liver failure in mice, indicating the therapeutic potential of iPSCs for liver diseases. Thus, we aim to investigate whether hiPSCs can prevent the malignant transformation of liver cancer.

Of particular interest is the finding from a miRNA microarray screening of specific PSC hepatocyte-like cells generated from patients with coronary heart disease, which revealed differential expression of miR-122-5p.[11] miRNAs are a group of non-coding RNAs ranging in size from 20 to 23 nucleotides that control the expression of downstream target genes by binding to their 3'-UTR structures. They represent viable targets for recently developed cancer therapies.[12] It has been shown that aberrant miRNA expression may serve as a possible biomarker for liver cancer and is associated with an unfavorable outcome in affected patients.[13] A recent study has identified miR-122-5p as a predictive marker for the prognosis of hepatocellular carcinoma (HCC).[14] Meanwhile, Tao *et al.*[15] have discovered that miR-122-5p potentially acts as a tumor suppressor in intrahepatic cholangiocarcinoma (ICC). Additionally, miR-122-5p overexpression inhibited citrate synthase to reduce proliferation, migration and invasion of nasopharyngeal carcinoma cells.[16] These findings suggest that miR-122-5p is a potential target that is expected to prevent the growth of liver cancer. However, the precise role of miR-122-5p in the treatment of liver cancer is not yet fully understood. Therefore, we aim to study how modulating miR-122-5p in hiPSCs affects the progression of liver cancer at the cellular level.

Against this background, it is evident that inducing hiPSCs to differentiate into hepatocyte-like cells represents a promising strategy to halt the progression of liver cancer. In this study, we aimed to investigate the role of miR-122-5p in regulating the differentiation of hiPSCs, as well as the effects of miR-122-5p-modified hiPSCs on the EMT and malignant transformation of liver cancer cells.

Materials and Methods

Cell culture

The hiPSCs were obtained from Ubigene Biotechnology Co., Ltd. (Guangzhou, China). HepG2 cells were acquired from Procell Life Science & Technology Co., Ltd. (Wuhan, China). HiPSCs were cultured in EZ stem™ stem cell complete culture medium (Ubigene Biotechnology). When the cells grew to 70%-80%, EZ stem cell digestion solution (Ubigene Biotechnology) was added and incubated with the cells for 3 min. Until most of the cells showed significant retraction under the microscope, the culture medium was replaced with fresh EZ stem cell culture medium and the cell suspension was obtained by gently blowing. Cells were passaged in a certain proportion. HepG2 cells were cultured in minimum essential medium (MEM; containing NEAA) medium (Pricella, Wuhan, China) containing 20% fetal bovine serum (FBS; Excell Bio, Suzhou, China), 50 units/mL streptomycin (Beyotime, Shanghai, China), and 100 units/mL penicillin at 37°C in a 5% CO_2 environment. When the cell density reached over 80%, the cells were digested with 1 mL of 0.25% trypsin (Gibco, Rockville, MD, USA) for 1 min. After the cells floated and became round, 5 mL of complete culture medium was added to terminate the digestion. Cells were then passaged at a 1:3 ratio. A co-culture system of hiPSCs and HepG2 cells was constructed using indirect contact method. Well-grown hiPSCs were inoculated into the top layer of Transwell at a concentration of 1×10^6 cells per well and cultured with EM stem cell culture medium. Then, HepG2 cells in logarithmic growth phase were seeded into the lower layer of the suitable chamber on a 6-well plate at a concentration of 1×10^6 per well and cultivated with MEM medium. In order to create a co-culture environment for hiPSCs and HepG2 cells, it was necessary to allow the liquid culture medium in the upper and lower layers of the chamber in contact.

Immunofluorescence

Immunofluorescence was used to detect the expression level of each marker and to assess the colocalization of N-Cadherin and E-Cadherin. Cells were seeded into a 6-well plate with a density of 1×10^6 cells per well and then treated according to the assigned groups. After washing with phosphate-buffered saline (PBS), cells were fixed with 4% paraformaldehyde (Beyotime) for 20 min. Following that, cells were exposed to 0.25% Triton X100 (Beyotime) for 20 min. After that, cells were blocked with goat serum (Bioss, Wuhan, China) for 30 min. After removing the blocking solution, cells were incubated at 4°C overnight with primary antibodies against octamer-binding transcription factor 4 (OCT4; ab181557, 1:250 dilution; Abcam, Cambridge, UK), SRY-box transcription factor 2 (SOX2; ab92494, 1:200 dilution; Abcam), Nanog homeobox (NANOG; ab109250, 1:250 dilution; Abcam). For the simultaneous immunodetection of two antigens, primary antibodies raised in different host species were used to avoid cross-reactivity. The primary antibodies and their specifications are as follows: albumin (ALB): mouse monoclonal antibody (ab19194, 1:500 dilution; Abcam); ASGPR: rabbit monoclonal antibody (ab254262, 1:100 dilution; Abcam); E-cadherin: mouse monoclonal antibody (ab1416, 1:200 dilution; Abcam); N-cad-

herin: rabbit monoclonal antibody (ab18203, 1:100 dilution; Abcam). The next day, species-specific secondary antibodies were applied: Alexa Fluor® 488-conjugated goat anti-mouse IgG (H&L) (ab150113, 1:500 dilution; Abcam) or Alexa Fluor® 594-conjugated goat anti-rabbit IgG (H&L) (ab150080, 1:400 dilution; Abcam). Secondary antibodies were incubated for 1 h in darkness at room temperature. Nuclei were counterstained with 4′,6-diamidino-2-phenylindole (DAPI) for 3 min. Negative controls were performed by omitting primary antibodies and replacing them with PBS. All experiments were independently repeated three times. Fluorescence images were captured using an EVOS M5000 fluorescence microscope (Thermo Fisher, Waltham, MA, USA), and ImageJ software was employed to analyze fluorescence intensity.

Cell transfection

HiPSCs were inoculated into a 6-well plate with a density of 1×10^6 cells per well. The miR-122-5p mimic, miR-122-5p inhibitor, mimic negative control (NC) and inhibitor NC were synthesized by Ribobio Co., Ltd. (Guangzhou, China). 5 µL of mimic NC (NC(+) group), inhibitor NC (NC(-) group), miR-122-5p mimic (miR-122-5p(+) group) or miR-122-5p inhibitor (miR-122-5p(-) group) was added to 120 µL of riboFECT CP Buffer and 12 µL of riboFECT CP Reagent (Ribobio Co.) and incubated for 15 min to form the carrier-lipid complex. Subsequent experiments were conducted after co-incubation of plasmids and cells for 48 h.

CCK8 assay

The CCK8 Kit (Bioss) was utilized to measure the proliferative capacity of cells. Cells in logarithmic growth phase were seeded into a 96-well plate (2×10^3 cells/well). Ten µL CCK8 solutions were used to treat cells for 2 h. With the aid of an RT-6000 microplate reader (Rayto, China), absorbance at 450 nm was recorded. The rate of cell survival was used to indicate cell proliferation. The calculation formula was as follows: cell survival rate (%) = (OD value (sample) - OD value (CCK8)) / (OD value (control group) - OD value (CCK8)) × 100%.

Detection of hepatocyte markers

The positive expression rate of ASGPR, a hepatocyte-specific surface receptor with broad applications in hepatocyte identification, functional assessment, and liver cancer diagnosis, was detected by flow cytometry. Cells grown in the logarithmic phase were placed into a 6-well plate at a concentration of 1×10^6 cells per well and cultured for 24 h. Then, cells were digested with trypsin and collected by centrifugation at 1000 rpm for 5 min. After rinsing with PBS, the obtained single-cell suspension was incubated with ASGPR antibody (ab254262, 1:500 dilution; Abcam) for 60 min in darkness at room temperature. After incubation, cells were washed with PBS and incubated with goat anti-rabbit IgG secondary antibody (ab6717, 1:1000 dilution; Abcam) for 30 min away from light. Then, cells were washed 2-3 times with PBS for 5 min each time and centrifuged to remove unbound antibody. Cells were resuspended in 300 µL PBS and transferred to a flow-through tube. Finally, the fluorescence was detected within 1 h using a flow cytometer (BD FACSCanto II; BD Biosciences, Franklin Lakes, NJ, USA) and the results of three independent replicates were analyzed using Flow jo software.

RT-PCR analysis

The cell/tissue total RNA isolation kit V2 (Vazyme, Nanjing, China) was employed to extract the total RNA from cells cultured in a six-well plate. By washing, precipitating, and separating the chloroform phase, pure RNA was obtained. Nano 600 (Jiapeng, China) was used to measure the RNA concentration and purity. The following experiments were performed utilizing RNA that had an A260/280 ratio of 1.9 to 2.1. Subsequently, the HiScript lll 1st Strand cDNA Synthesis Kit (Vazyme) was used to obtain cDNA. Then, Taq Pro Universal SYBR qPCR Master Mix (Vazyme) was added to a real-time quantitative PCR reaction system. The following steps were then followed to detect the results using a CFX96 Touch 1855195 Real time Fluorescence Quantitative PCR Instrument (Bio-Rad, Hercules, CA, USA): pre-denaturation for 10 min at 95°C, denaturation for 15 s at 95°C, annealing for 30 s at 58°C, extension for 30 s at 72°C, for 40 cycles; Melting curve: 95°C for 15 s, 60°C for 60 s, 95°C for 15 s. Relative primer (Shanghai Sangon Co., Ltd., Shanghai, China) sequences were as follows: ALB (Forward: GGGGTGTGTTTCGTCGAGAT; Reverse: AGGCAATCAACACCAAGGCT); hepatocyte nuclear factor 4alpha (HNF4α; Forward: ACCTCAGCAACGGACAGATG; Reverse: AGAGGGGCTTGACGATTGTG); cytokeratin 18 (CK18; Forward: CCTGCTGAACATCAAGGTCAA; Reverse: CTATCCGGCGGGTGGT); E-Cadherin (Forward: TACCCTGGTGGTTCAAGCTG; Reverse: CAAAATCCAAGCCCGTGGTG); N-Cadherin (Forward: GGCGTTATGTGTGTATCTTCACT; Reverse: GCAGGCTCACTGCTCTCATA); GAPDH (Forward: TCCAAAATCAAGTGGGGCGA; Reverse: AAATGAGCCCCAGCCTTCTC). The results was calculated by $2^{-\Delta\Delta Ct}$. GAPDH was used to adjust each gene's expression.

Western blot

Western blot analysis was employed to determine the expression of N-Cadherin and E-Cadherin. In a nutshell, total proteins were extracted using RIPA lysis buffer (Beyotime, Shanghai, China) and the protein concentrations were examined using a bicinchoninic acid (BCA) kit (NCM Biotech, Shanghai, China). 20 µg in each sample was separated by SDS-PAGE gel and subsequently transferred to a polyvinylidene fluoride membrane (Millipore, Billerica, MA, USA). The membranes were blocked with 5% skim milk powder (BD Biosciences) and then incubated for a whole night at 4°C with anti-E-Cadherin (ab40772, 1:10000 dilution; Abcam), anti-N-Cadherin (ab18203, 1 µg/mL; Abcam), and anti-GAPDH antibodies (ab9485, 1:1000 dilution; Abcam). After washing, the membranes were probed with goat anti-rabbit IgG H&L/HRP secondary antibody (bs-0295G-HRP, 1:5000 dilution; Bioss) at room temperature for 1 h. Finally, the membranes were developed using a chemiluminescence imaging system (Tanon, Shanghai, China), and the grayscale values were analyzed using ImageJ software.

Transwell assay

A Transwell chamber coated with matrix gel was filled with a suspension of HepG2 cells at a specific concentration of $1\text{-}5\times10^5$ cells/mL. Medium (600 µL) containing 10% FBS was added to the lower chamber. 4% paraformaldehyde was used to fix cells for 10 min. The fixed solution in the bottom chamber was then discarded, the top chamber was removed, and crystal violet staining solution (Sigma-Aldrich, St. Louis, MO, USA) was added. The chambers were submerged in the staining solution for 10 min. The upper chamber was allowed to dry naturally after staining and washed thoroughly with water. A microscope was used to examine the images.

Wound healing assay

HepG2 cells were placed in a 6-well plate with a specific concentration of 1×10^6 cells/well and incubated for 4 h. When the cell growth reached more than 90%, the line indicated on the back of the plate was then vertically pressed with a pipette tip to create a scratch. The results were examined under a microscope, and the size of the cell scratch at 0 h was recorded. This information was repeated after 24 h of culture.

Detection of cell apoptosis

To assess the apoptosis rate of HepG2 cells, the AnnexinV-FITC kit (Beyotime) was used in this study. When the cells had grown to cover the walls of the monolayer bottle, they were centrifuged and re-suspended at 1000 rpm for 5 min. The prepared 1X solution of Annexin V binding was then mixed with the cell suspension to a final density of 1×10^6 cells/mL. 5 μL of AnnexinV-FITC complex and 5 μL of propidium iodide (PI) solution were added to 100 μL of cell suspension and incubated for 15 min in darkness at room temperature. Next, 1X Annexin V binding solution (400 μL) was added. Finally, the fluorescence was detected within 1 h using an Attune NxT flow cytometry (Invitrogen), and data were examined using Flow-Jo software.

Statistical analysis

The experimental data expressed as mean ±SEM were processed and statistically analyzed using GraphPad Prism 8 (La Jolla, CA, USA). Comparison of the sample means of multiple groups was performed by the analysis of variance (ANOVA), and comparison of the sample means of two groups was conducted by a *t*-test. A *p*-value below 0.05 is a sign of a significant statistical difference.

Results

Culture and identification of hiPSCs

HiPSCs were cultured in vitro using a non-feeding layer method, which involved inoculating them into culture dishes coated with Matrigel on the surface. Tightly packed multicellular colonies with distinct borders were formed by the aggregation of cells, and healthy colonies merged and linked fluidly (Figure 1A). Then, we further assessed the pluripotency of this cell line by detecting the expression of proteins linked to stem cell pluripotency. As shown by immunofluorescence staining, transcription factors (OCT4, SOX2) and nuclear protein (NANOG), which are specific markers of stem cells, were strongly expressed in hiPSCs (Figure 1B). These results confirmed that this hiPSC cell line exhibited self-renewal characteristics and pluripotency, and laid a solid experimental foundation for subsequent differentiation of hiPSCs into hepatocyte-like cells.

Overexpression of miR-122-5p induced differentiation of hiPSCs into hepatocyte like-cells.

To investigate the impact of miR-122-5p on hiPSCs, we constructed plasmids for miR-122-5p overexpression and knockdown, and transfected them into hiPSCs. We found that the proliferation ability of hiPSCs was enhanced following upregulation of miR-122-5p, whereas it was significantly weakened after downregulation of miR-122-5p (Figure 2A). Next, we examined the positive expression rate of liver cell marker ASGPR to assess the induction efficiency of miR-122-5p. Flow cytometry analysis revealed that miR-122-5p overexpression increased ASGPR positive expression in hiPSCs, while knockdown of miR-122-5p had the opposite effect (Figure 2 B,C). Besides, immunofluorescence staining showed high expression of liver cell markers, including ASGPR, ALB, and AFP, in miR-122-5p-overexpressing modified hiPSCs (Figure 2 D-G). Furthermore, we detected the levels of liver-cell specific genes, including ALB, HNF4α, and CK18. The real-time PCR analysis demonstrated a significant increase in the expression levels of these genes after miR-122-5p upregulation (Figure 2H). Collectively, our data suggest that miR-122-5p overexpression promotes the survival and acquisition of hepatocyte-like cell characteristics in hiPSCs.

MiR-122-5p modified hiPSCs alleviated malignant transformation of HepG2 liver cancer cell phenotype

Based on the above results, hiPSCs exhibited enhanced proliferation ability and liver cell characteristics following miR-122-5p overexpression. To evaluate whether this differentiation could help improve liver cancer, we co-cultured hiPSCs with HepG2 cells. The CCK8 experiment demonstrated that overexpression of miR-122-5p in hiPSCs led to the inhibition of the proliferation capacity of HepG2 cells while hiPSCs transfected with miR-122-5p knockdown plasmids promoted the proliferation of HepG2 cells (Figure 3A). Additionally, the Transwell and wound healing assays demonstrated a notably reduction in the invasion and migration capabilities of HepG2 cells when co-cultured with miR-122-5p-overexpressing hiPSCs. Furthermore, as illustrated by flow cytometry, miR-122-5p-overexpressing hiPSCs also induced an increased rate of apoptosis in HepG2 cells (Figure 3 B-G). Overall, these findings suggest that the differentiation of hiPSCs to hepatocyte-like cells promoted by miR-122-5p contributes to the amelioration of malignant liver cancer progression.

MiR-122-5p modified hiPSCs arrested EMT of HepG2 liver cancer cells.

Given the critical role of EMT in promoting the migration and invasion of liver cancer cells, we further examined the impact of miR-122-5p-overexpressing hiPSCs on the EMT process in HepG2 cells. We focused on the expression of E-Cadherin and N-Cadherin, which are two key molecules in the process of EMT. The real-time PCR analysis showed a notable increase in E-Cadherin levels and a decrease in N-Cadherin levels in HepG2 cells co-cultured with miR-122-5p-overexpressing hiPSCs. In contrast, HepG2 cells treated with miR-122-5p-silenced hiPSCs exhibited downregulated E-cadherin expression and upregulated N-cadherin expression (Figure 4A). These results were further confirmed by the western blot assay (Figure 4 B,C). Besides, miR-122-5p-overexpressing hiPSCs increased E-Cadherin fluorescence intensity and reduced N-Cadherin fluorescence intensity in HepG2 cells (Figure 4 D-F). These findings demonstrate that miR-122-5p-induced hepatocyte-like differentiation of hiPSCs suppressed the progression of EMT, which may underlie its inhibitory effect on liver cancer.

Discussion

In recent years, stem cells have attracted attention in cell replacement therapy research due to their ability to differentiate into different types of tissue cells, and are expected to provide new sources of liver cells for artificial liver therapy.[17] The currently reported stem cells include mesenchymal stem cells, pluripotent stem cells, and liver progenitor cells.[18-20] In the present research, we revealed that hiPSCs, a type of stem cell with efficient and directional differentiation potential, could ameliorate the malignant conversion of liver cancer by acquiring hepatocyte-like its characteristics. Furthermore, we firstly identified miR-122-5p as a driving molecule that induced hiPSCs to differentiate into hepatocyte-like cells.

Since the first reported discovery, hiPSCs have laid a new foundation for cell therapy and drug development and have progressively advanced into the clinical application stage. Numerous studies have confirmed that hiPSCs can be directed to differentiate into various cell lineages.[21] In this study, hiPSCs were obtained from healthy male neonatal foreskin cells. HiPSCs are a type of cell that reprograms and differentiates to become similar to embry-

onic stem cells through the introduction of a specific set of four transcription factors (SOX2, OCT4, Klf4 and Cmyc or SOX2, OCT4, NANOG and LIN28) into cells. SOX2 and OCT4 are not only core transcription factors for somatic reprogramming into iPSCs, but also play crucial roles in maintaining cellular self-renewal and pluripotency.[22] In the hiPSCs used in this study, SOX2, OCT4, and NANOG were all highly expressed, ensuring their differentiation potential and stability in our subsequent experiments.

A growing body of studies has proven that miRNAs play important roles in the malignant process of liver cancer.[23,24] For instance, miR-557 inhibits the proliferation and migration of HCC cells by downregulating CBX4.[25] By regulating SIRT1, miR-4461 suppresses liver cancer stem cell expansion and chemoresistance.[26] Research has shown that introducing miRNAs can increase the formation of iPSC colonies and promote their differentiation and proliferation.[27] It has been noted that the miR-122-5p expression is increased in iPSC-HLCs (hepatocyte-like cells) from patients with stable coronary heart disease.[11] This suggests that miR-122-5p is involved in the differentiation of iPSCs into hepatocyte-like cells. Inspired by these findings, we transfected hiPSCs with miR-122-5p mimic and inhibitor plasmids to upregulate and downregulate miR-122-5p expression, respectively. We found that overexpression of miR-122-5p increased the proliferative capacity of hiPSCs. This indicated that miR-122-5p maintained hiPSCs in an active state, thereby increasing and ensuring the probability of successful differentiation. Afterwards, we detected the expression of liver cell markers in hiPSCs using various methods and found that these markers were highly expressed in hiPSCs transfected with miR-122-5p overexpressing plasmids. These results supported our

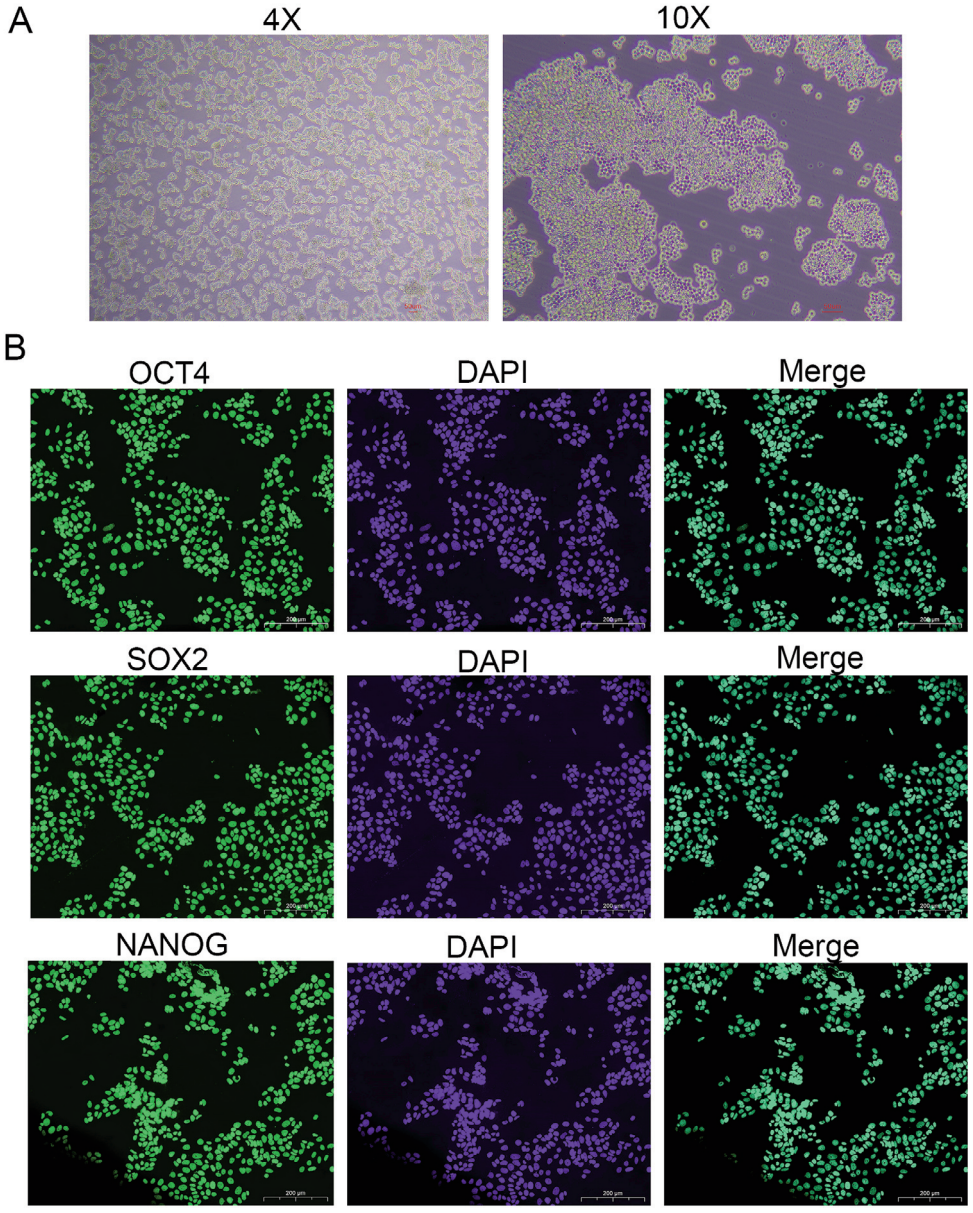

Figure 1. Identification of hiPSCs. **A**) A microscope at 40x and 100x magnification to observe the morphology of hiPSCs; scale bar: 50 µm. **B**) Immunofluorescence staining for the expression of stem cell specific protein markers OCT4, SOX2, and NANOG in iPSCs; green indicates OCT4, SOX2, or NANOG staining, blue indicates DAPI staining of the cell nucleus, and merge is a synthetic image; scale bar: 200 µm. All experimental data were presented as mean ± SEM from three independent replicate experiments (n=3).

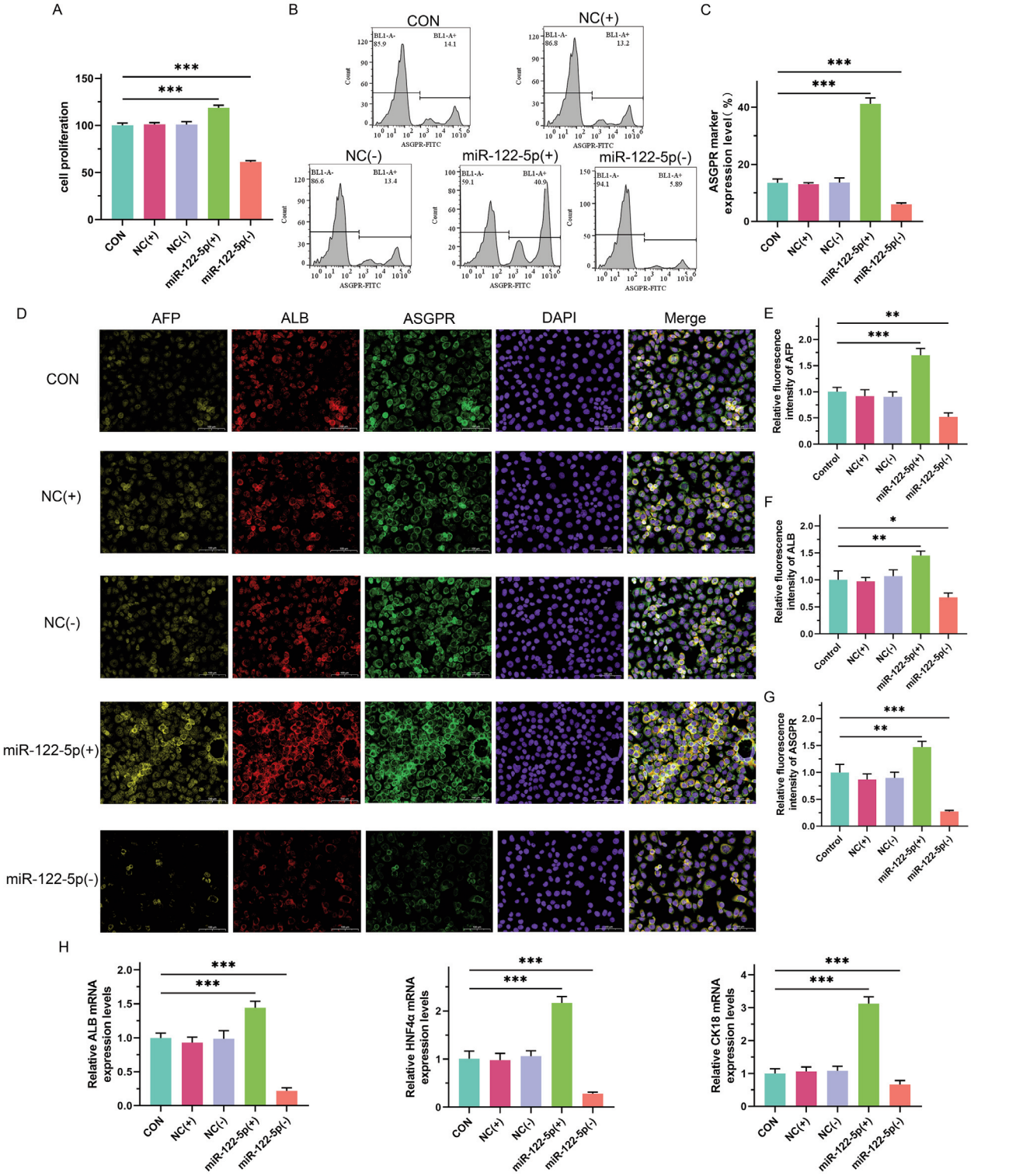

Figure 2. The effect of miR-122-5p overexpression or knockdown on the differentiation of iPSCs into hepatocyte-like cells. **A**) CCK8 assay for the changes in cell proliferation ability. **B**) Flow cytometry for the positive expression rate of liver cell marker, ASGPR. **C**) Quantitative analysis of the expression level of ASGPR. **D**) Immunofluorescence staining for the expression of liver cell markers AFP, ALB, and ASGPR; yellow indicates AFP staining, red indicates ALB staining, green indicates ASGPR staining, blue indicates DAPI staining of the cell nucleus, and Merge is a synthetic image of AFP, ALB, ASGPR and DAPI staining; scale bar: 100 μm. **E-G**) Quantitative analysis of the expression levels of AFP, ALB, and ASGPR. **H**) Real-time PCR assay for the expression levels of liver cell specific genes, ALB, HNF4α and CK18. For the CON group, hiPSCs were conventionally cultured without any other treatment. For the NC(+) group, hiPSCs were transfected with control mimic vector. For the NC(-) group, hiPSCs were transfected with control inhibitor vector. For the miR-122-5p(+) group, hiPSCs were transfected with miR-122-5p mimic. For the miR-122-5p(-) group, hiPSCs were transfected with miR-122-5p inhibitor. All experimental data were presented as mean ± SEM from three independent replicate experiments (n=3). *p<0.05, **p<0.01, ***p<0.001.

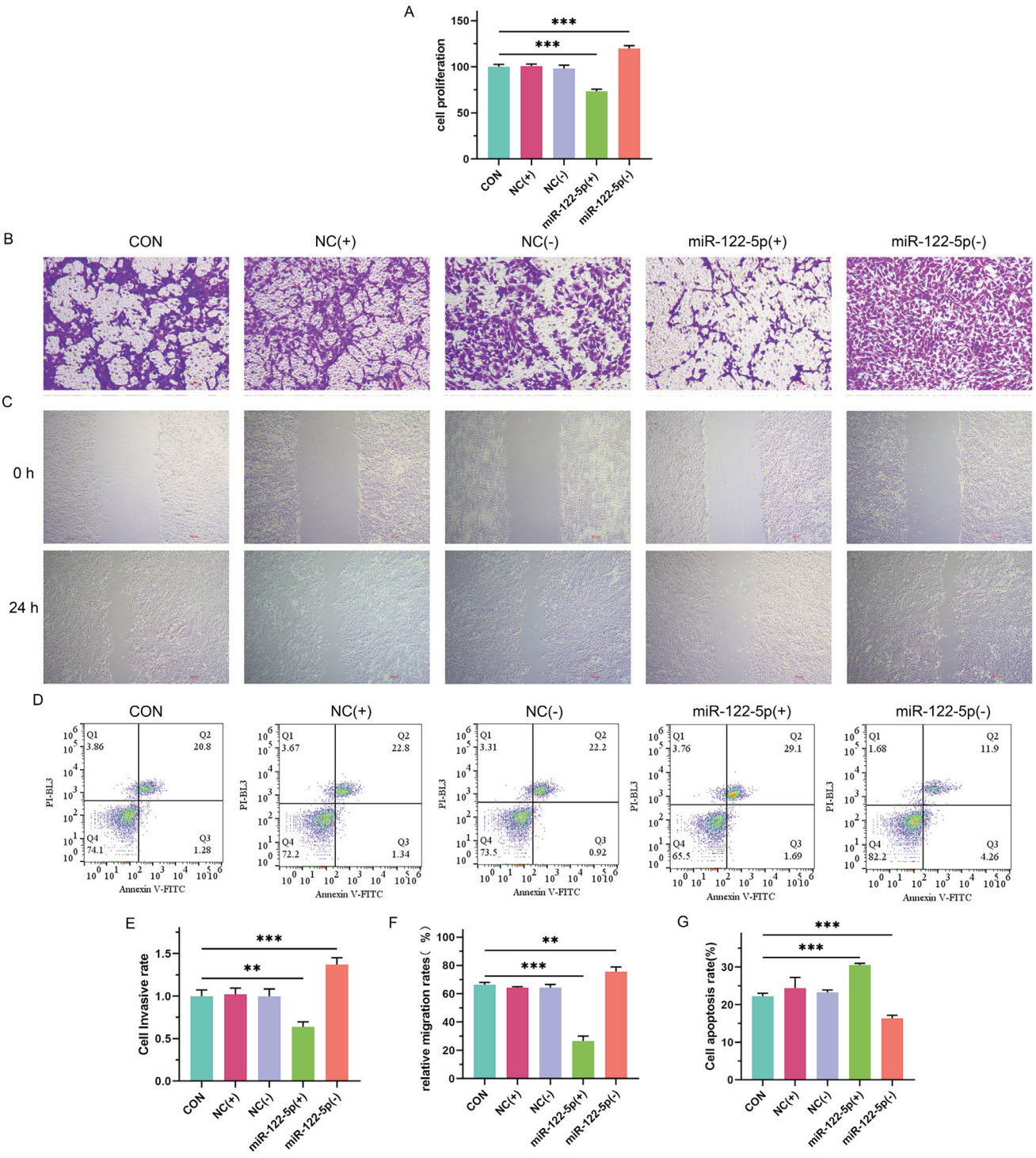

Figure 3. The effect of miR-122-5p modified iPSCs on the phenotype malignant transformation of HepG2 liver cancer cells. **A**) CCK8 assay for the changes in cell proliferation ability. **B**) Transwell assay for the changes in cell invasion ability; scale bar: 50 μm. **C**) Wound healing assay for the migration ability of cells at 24 h; scale bar: 50 μm. **D**) Flow cytometry to detect the apoptosis rate of cells. **E**) The quantitative analysis of cell invasion ability. **F**) The quantitative analysis of cell migration ability. **G**) The quantitative analysis of the apoptosis rate. For the CON group, hiPSCs were co-cultured with HepG2 cells without any other treatment. For the NC(+) group, control mimic vector was transfected into the co-culture system of iPSCs and HepG2 cells. For the NC(-) group, control inhibitor vector was transfected into the co-culture system of iPSCs and HepG2 cells. For the miR-122-5p(+) group, miR-122-5p mimic was transfected into the co-culture system of iPSCs and HepG2 cells. For the miR-122-5p(-) group, miR-122-5p inhibitor was transfected into the co-culture system of iPSCs and HepG2 cells. All experimental data were presented as mean ± SEM from three independent replicate experiments (n=3). $^{**}p<0.01$, $^{***}p<0.001$.

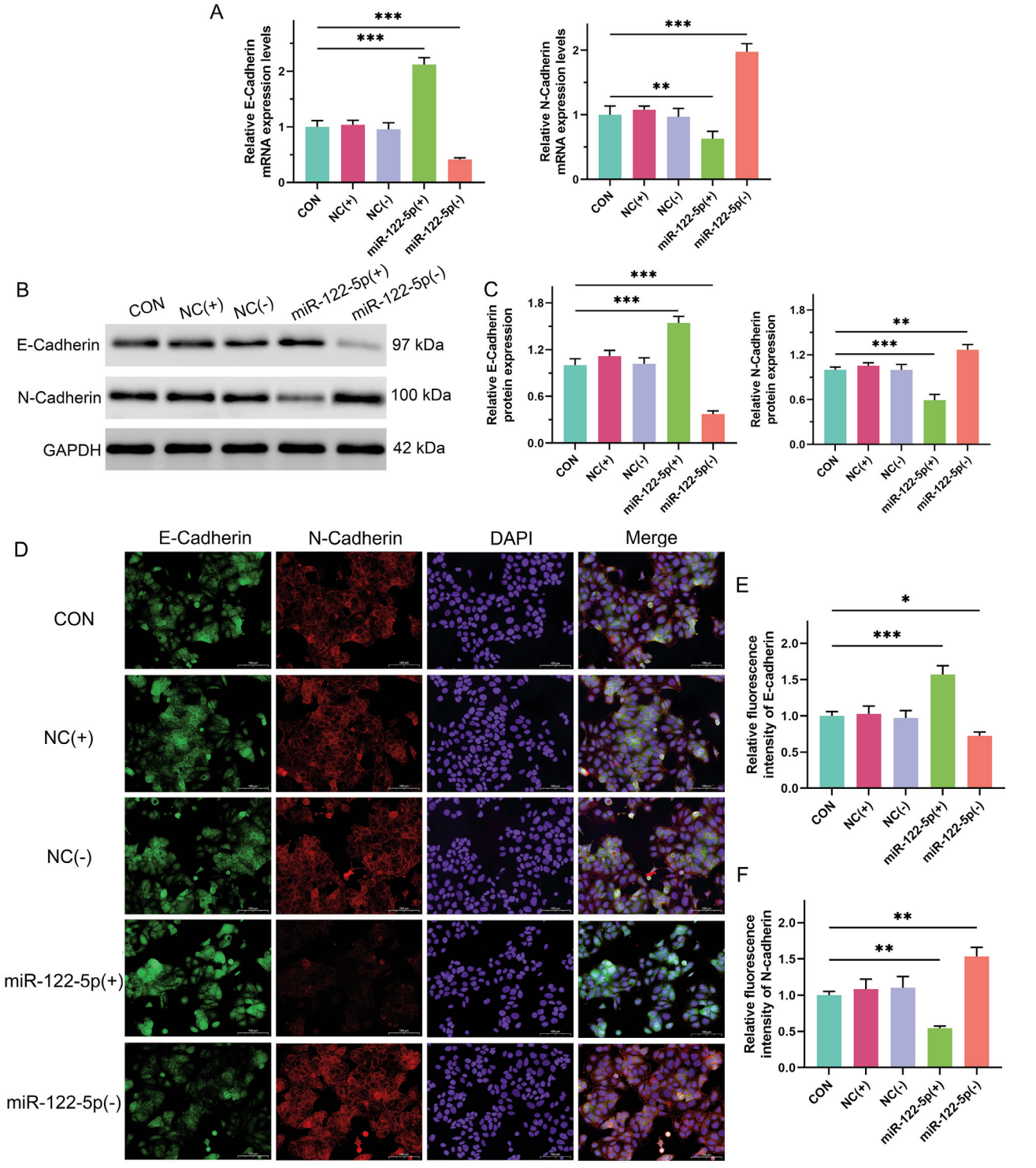

Figure 4. The effect of miR-122-5p modified iPSCs on epithelial mesenchymal transition in HepG2 liver cancer cells. **A**) RT-PCR for the mRNA expression levels of E-Cadherin and N-Cadherin in different groups. **B**) Western blot assay for the protein expression levels of E-Cadherin and N-Cadherin; GAPDH was set as a reference. **C**) Quantitative analysis of the protein expression levels of E-Cadherin and N-Cadherin. **D**) Immunofluorescence staining to observe the expression of E-Cadherin and N-Cadherin; green indicates E-Cadherin staining, red indicates N-Cadherin staining, blue indicates DAPI staining of the cell nucleus, and merge is a synthetic image of E-Cadherin, N-Cadherin and DAPI staining; scale bar: 100 μm. **E,F**) Quantitative analysis of fluorescence intensity of E-Cadherin and N-Cadherin. For the NC(-) group, control inhibitor vector was transfected into the co-culture system of iPSCs and HepG2 cells. For the miR-122-5p(+) group, miR-122-5p mimic was transfected into the co-culture system of iPSCs and HepG2 cells. For the miR-122-5p(-) group, miR-122-5p inhibitor was transfected into the co-culture system of iPSCs and HepG2 cells. All experimental data were presented as mean ±SEM from three independent replicate experiments (n=3). *p<0.05, **p<0.01, ***p<0.001.

hypothesis that miR-122-5p prompted the differentiation of hiPSCs into hepatocyte-like cells. As demonstrated above, we confirmed that hiPSCs acquired hepatocyte-like properties following miR-122-5p induction. Research has shown that liver cell transplantation can rapidly sustain liver biological activity and improve liver regeneration, making it a promising therapeutic approach for liver failure.[28,29] However, liver cells have a finite supply and are unable to sustain long-term viability. Therefore, we investigated whether hepatocyte-like hiPSCs could be utilized for liver cancer treatment. For this purpose, we co-cultured hiPSCs with HepG2 cells. According to our research, the invasion, migration, and survival capacities of HepG2 cells were greatly inhibited when co-cultured with miR-122-5p-overexpressing hiPSCs. These findings revealed the crucial role of hiPSCs and miR-122-5p in the treatment of liver cancer. The biological process known as EMT is linked to tumor metastasis and cancer progression. Strong cell connections, a regular morphology, barrier and secretory functions are characteristics of normal epithelial cells. However, following an EMT transition, cells lose their inherent polarity and gain greater migratory and invasive capacities, along with increased resistance to apoptosis and medication resistance.[30,31] It has been reported that the differentiation of hiPSCs into different types of cells leads to different results of EMT. For example, Mong *et al.*[32] have found that differentiation of iPSCs into trophoblast-like stem cells led to upregulation of EMT related gene expression. Nevertheless, the induction of iPSCs requires the involvement of mesenchymal-epithelial transition (MET), which contrasts with the EMT process.[33] Thus, we assessed whether miR-122-5p-overexpressing hiPSCs could influence the process of EMT. Our results showed that the epithelial cell surface marker E-Cadherin was upregulated and the mesenchymal cell marker N-Cadherin was downregulated following treatment with miR-122-5p-overexpressing hiPSCs, indicating that the improvement impacts of hiPSCs on liver cancer cells are related to inhibition of EMT. In addition, recent studies on differential gene analysis suggest future directions for our research, such as identifying miR-122-5p-regulated differentially expressed genes to reveal potential targets for liver cancer therapy.[34-36] In summary, our studies provide evidence that hiPSCs, differentiating into hepatocyte-like cells through miR-122-5p induction, prevent EMT process in liver cancer. According to our research, there is a strong correlation between miR-122-5p expression and the hepatocyte-like phenotype of hiPSCs. These findings provide important theoretical basis for targeted diagnosis and treatment of liver cancer, with significant clinical significance. The hiPSCs treated with miR-122-5p may serve as a novel cell source for treating end-stage liver failure. However, the current research is limited to the cellular level. Our conclusion needs to be validated at the animal level, and the deeper mechanisms also require more research.

References

1. Song C, Lv J, Yu C, Zhu M, Yu C, Guo Y, et al. Adherence to healthy lifestyle and liver cancer in Chinese: a prospective cohort study of 0.5 million people. Brit J Cancer 2022;126:815-21.
2. Anwanwan D, Singh SK, Singh S, Saikam V, Singh R. Challenges in liver cancer and possible treatment approaches. Biochim Biophys Acta Rev Cancer 2020;1873:188314.
3. Dongre A, Weinberg RA. New insights into the mechanisms of epithelial-mesenchymal transition and implications for cancer. Nat Rev Mol Cell Biol 2019;20:69-84.
4. Yoshida GJ. Emerging role of epithelial-mesenchymal transition in hepatic cancer. J Exp Clin Canc Res 2016;35:141.
5. Peng WC, Kraaier LJ, Kluiver TA. Hepatocyte organoids and cell transplantation: What the future holds. Exp Mol Med 2021;53:1512-28.
6. Rountree CB, Mishra L, Willenbring H. Stem cells in liver diseases and cancer: recent advances on the path to new therapies. Hepatology 2012;55:298-306.
7. Aboul-Soud M, Alzahrani AJ, Mahmoud A. Induced pluripotent stem cells (iPSCs)-roles in regenerative therapies, disease modelling and drug screening. Cells 2021;10:2319.
8. Poetsch MS, Strano A, Guan K. Human induced pluripotent stem cells: from cell origin, genomic stability, and epigenetic memory to translational medicine. Stem Cells 2022;40:546-55.
9. Xing Q, Luo Y, Gao Y, Zhang S, Zhu Z, Wang Y, et al. Hepatectomised patient sera promote hepatocyte differentiation of human-induced pluripotent stem cells. Digest Liver Dis 2014;46:731-7.
10. Yuan L, Zhang Y, Liu X, Chen Y, Zhang L, Cao J, et al. Agonist c-Met monoclonal antibody augments the proliferation of hiPSC-derived hepatocyte-like cells and improves cell transplantation therapy for liver failure in mice. Theranostics 2019;9:2115-28.
11. Alexanova A, Raitoharju E, Valtonen J, Aalto-Setala K, Viiri LE. Coronary artery disease patient-derived iPSC-hepatocytes have distinct miRNA profile that may alter lipid metabolism. Sci Rep-Uk 2023;13:1706.
12. Rupaimoole R, Slack FJ. MicroRNA therapeutics: towards a new era for the management of cancer and other diseases. Nat Rev Drug Discov 2017;16:203-22.
13. Ghafouri-Fard S, Honarmand TK, Hussen BM, Taheri M. MicroRNA signature in liver cancer. Pathol Res Pract 2021;219:153369.
14. Roa-Colomo A, Lopez GM, Molina-Vallejo P, Rojas A, Sanchez MG, Aranda-Garcia V, et al. Hepatocellular carcinoma risk-stratification based on ASGR1 in circulating epithelial cells for cancer interception. Front Mol Biosci 2022;9:1074277.
15. Tao L, Wang Y, Shen Z, Cai J, Zheng J, Xia S, et al. Activation of IGFBP4 via unconventional mechanism of miRNA attenuates metastasis of intrahepatic cholangiocarcinoma. Hepatol Int 2024;18:91-107.
16. Guo L, Wang Z, Fu Y, Wu S, Zhu Y, Yuan J, et al. MiR-122-5p regulates erastin-induced ferroptosis via CS in nasopharyngeal carcinoma. Sci Rep 2024;14:10019.
17. Li Y, Lu L, Cai X. Liver Regeneration and cell transplantation for end-stage liver disease. Biomolecules 2021;11:1907.
18. Hu C, Zhao L, Wu Z, Li L. Transplantation of mesenchymal stem cells and their derivatives effectively promotes liver regeneration to attenuate acetaminophen-induced liver injury. Stem Cell Res Ther 2020;11:88.
19. Kakinuma S, Nakauchi H, Watanabe M. Hepatic stem/progenitor cells and stem-cell transplantation for the treatment of liver disease. J Gastroenterol 2009;44:167-72.
20. Dianat N, Steichen C, Vallier L, Weber A, Dubart-Kupperschmitt A. Human pluripotent stem cells for modelling human liver diseases and cell therapy. Curr Gene Ther 2013;13:120-32.
21. Karagiannis P, Takahashi K, Saito M, Yoshida Y, Okita K, Watanabe A, et al. Induced pluripotent stem cells and their use in human models of disease and development. Physiol Rev 2019;99:79-114.
22. Ding Y, Yuan X, Zou Y, Gao J, Xu X, Sun H, et al. OCT4, SOX2 and NANOG co-regulate glycolysis and participate in somatic induced reprogramming. Cytotechnology 2022;74:371-83.
23. Xia M, Chen J, Hu Y, Qu B, Bu Q, Shen H. miR-10b-5p pro-

motes tumor growth by regulating cell metabolism in liver cancer via targeting SLC38A2. Cancer Biol Ther 2024; 25:2315651.
24. Olarewaju O, Hu Y, Tsay HC, Yuan Q, Eimterbäumer S, Xie Y, et al. MicroRNA miR-20a-5p targets CYCS to inhibit apoptosis in hepatocellular carcinoma. Cell Death Dis 2024;15:456.
25. Sun X, Ding W, Jiang C, Fang Z. MiR-557 suppresses hepatocellular carcinoma cell proliferation and migration via downregulating CBX4. BIOCELL. 2024;48:1071-9.
26. Yang D, Zhang P, Yang Z, Hou G, Yang Z. miR-4461 inhibits liver cancer stem cells expansion and chemoresistance via regulating SIRT1. Carcinogenesis 2024 45:463-74.
27. Salloum-Asfar S, Abdulla SA, Taha RZ, Thompson IR, Emara MM. Combined noncoding RNA-mRNA regulomics signature in reprogramming and pluripotency in iPSCs. Cells 2022;11:3833.
28. Li F, Wei H, Jin Y, Xue T, Xu Y, Wang H, et al. Microfluidic fabrication of microRNA-induced hepatocyte-like cells/human umbilical vein endothelial cells-laden microgels for acute liver failure treatment. Acs Nano 2023;17:25243-56.
29. Yoshimoto K, Maki K, Adachi T, Kamei KI. Cyclic stretching enhances angiocrine signals at liver bud stage from human pluripotent stem cells in two-dimensional culture. Tissue Eng Pt A 2024;30:426-39.
30. Davis FM, Stewart TA, Thompson EW, Monteith GR. Targeting EMT in cancer: opportunities for pharmacological intervention. Trends Pharmacol Sci 2014;35:479-88.
31. Sabouni E, Nejad MM, Mojtabavi S, Khoshduz S, Mojtabavi M, Nadafzadeh N, et al. Unraveling the function of epithelial-mesenchymal transition (EMT) in colorectal cancer: Metastasis, therapy response, and revisiting molecular pathways. Biomed Pharmacother 2023;160:114395.
32. Mong EF, Yang Y, Akat KM, Canfield J, VanWye J, Lockhart J, et al. Chromosome 19 microRNA cluster enhances cell reprogramming by inhibiting epithelial-to-mesenchymal transition. Sci Rep-Uk 2020;10:3029.
33. Unternaehrer JJ, Zhao R, Kim K, Cesana M, Powers JT, Ratanasirintrawoot S, et al. The epithelial-mesenchymal transition factor SNAIL paradoxically enhances reprogramming. Stem Cell Rep 2014;3:691-8.
34. Dong H, Yin C, Xiao D, Tang Y. Identification of differentially expressed genes to predict the risk of heart failure in older patients with hypertrophic cardiomyopathy. Aging (Albany NY) 2024;16:10860-7.
35. Yu Z, Song L, Wang Y, Chen X, Chen P, Zhong S, et al. Integrating bulk-RNA and single-cell analysis reveals heterogeneous expression of cuproptosis-related sorafenib-resistant genes in hepatocellular carcinoma. Oncologie 2024;26: 783-97.
36. Sensi B, Angelico R, Toti L, Conte L, Coppola A, Tisone G, et al. Mechanism, potential, and concerns of immunotherapy for hepatocellular carcinoma and liver transplantation. Curr Mol Pharmacol 2024;17:e18761429310703.

Received: 24 January 2025. Accepted: 2 April 2025.

European Journal of Histochemistry 2025; 69:4190
doi:10.4081/ejh.2025.4190